IC/88/252

INTERNATIONAL CENTRE FOR THEORETICAL PHYSICS

STANDING SHOCKS IN ADIABATIC BLACK HOLE ACCRETION OF ROTATING MATTER

Marek A. Abramowicz

and

Sandip K. Chakrabarti

INTERNATIONAL ATOMIC ENERGY AGENCY

UNITED NATIONS EDUCATIONAL, SCIENTIFIC AND CULTURAL ORGANIZATION

IC/88/252

International Atomic Energy Agency
and
United Nations Educational Scientific and Cultural Organization
INTERNATIONAL CENTRE FOR THEORETICAL PHYSICS

STANDING SHOCKS IN ADIABATIC BLACK HOLE ACCRETION OF ROTATING MATTER *

Marek A. Abramowicz
International School for Advanced Studies, Trieste, Italy
and
International Centre for Theoretical Physics, Trieste, Italy

and

Sandip K. Chakrabarti
International Centre for Theoretical Physics, Trieste, Italy.

ABSTRACT

We present all the solutions for stationary, axially symmetric, transonic, adiabatic flows with polytropic, rotating fluid configurations of small transverse thickness, in an arbitrarily chosen potential. Special attention is paid to the formation of the standing shocks in the case of black hole accretion and winds. We point out the possibility of three types of shocks depending upon three extreme physical conditions at the shocks. These are: Rankin-Hugoniot shocks, isentropic compression waves, and isothermal shocks. We write down the shock conditions for these three cases and discuss breifly the physical situations under which these shocks may form. A complete discussion on the properties of these shocks will be presented elsewhere.

MIRAMARE – TRIESTE

August 1988

* Submitted for publication.

1 Introduction

This paper is the first in a series devoted to a systematic study of the axially symmetric standing shocks in the black hole accretion disks and winds. Although the previously published papers in this subject provided many important details, a global understanding of the role of the different types of shocks in different astrophysical situations involving rotating matter was missing. The series will present all the possible solutions for stationary, axially symmetric, transonic flows of rotating polytropic matter with small vertical thickness and with dissipation very small except at the shocks.

A physically realistic model for such flows should be at least two dimensional and it should include the dissipation, the radiative transfer, and the realistic equation of state. Equations describing it are too difficult to solve however, and for this reason all the authors who previously studied shocks in accretion flows have always adopted some kind of approximations.

Chang and Ostriker (1985) included in their model of shocks quite realistic equation of state and some effects of dissipation, but have *neglected rotation*. Their model was spherically symmetric, i.e. one dimensional. Another set of studies of shocks in the non-rotating flows was made by Ferrari *et al.* (1985) and the references therein. In these works sevaral cases were presented where shocks are produced by varying the flow boundary or by sudden deposition of momentum into the flow.

All the works which treated black hole accretion flows or winds including rotation assumed strictly *no dissipation* outside the shocks. All of them have also neglected the possibility that dissipation may occur not only accross, but also from the upper and the lower "surfaces" of the shock to the surrounding medium through radiative losses. In particular, Hawley, Smarr and Wilson (1984) and Hawley (1986) constructed numerically a few examples of polytropic shocks in a fully two-dimensional flow accreting *supersonically* at the outer boundary of the grid. Such an inflow is not necessarily realistic it cannot provide a global view of shock formation could not be obtained from such works. A rather important step in this regard was taken by Fukue (1987) who constructed one example of standing shock in the accretion flow with a realistic equation of state by connecting a pair of shock free transonic solutions. His work in addition to the restrictions mentioned before, assumed a rigid flow surface (conical) which means that the flow was *not* in a vertical equlibrium and therefore it was, in a sense, only one dimensional.

The above examples give a complete list of the general types of the *axially symmetric* models of shocks which have been studied (but *not* a complete list of papers). Non-axially symmetric shocks have been recently discussed in a series of papers initiated by Sawada *et al.* (1987) and Spruit (1987). These spiral shocks dissipate angular momentum and provide a torqe which leads to accretion of rotating matter even in the absence of viscosity. Numerical simulations of spiral shocks by Kaisig (1988) support this assertion.

Our model allows, *unlikely* all the other models discussed so far, the radiative losses from the upper and the lower surfaces of the shock and because of this it can describe parametrically *any* possible dissipation mechanism at the shock. Like other works, it assumes strictly no dissipation *outside* the shocks. Our model is more accurate than all the models which assume *apriori* the shape of the flow, because it consistently computes the shape by assuming the approximate condition of the vertical equilibrium using the so called 1.5D (one-and-a-half dimensional) method in which all the relevant equations of hydrodynamics are vertically integrated. The treatment of the radial equations is fully consistent, but the equations in the transverse direction are only half-dimensionally correct: the vertical equilibrium condition is considered, but

the motion along this direction is neglected. Thus, the vertically integrated black hole accretion flow models are in the above sense 1.5 dimensional. Contrary to this, the numerical method of Hawley *et al.* is fully 2D. However, our analytic models do not differ very much from the corresponding numerical 2D models. In addition our method gives the global and *complete* picture of all the possible solutions, while the numerical 2D methods can provide only isolated examples.

In the present paper of the series, we write down all the basic equations of the model including the transonic condition at the critical points and the shock conditions. We point out the possibility of three types of shocks: Rankin-Hugoniot shocks, isentropic compression waves and isothermal shocks, consistent with three extreme dissipation processes occuring at the shock. Outside the shock the flow is dissipation free. In the second paper of this series (Chakrabarti 1988, hereafter referred to as Paper II), we study in detail the properties of these shocks. We divide the whole parameter space spanned by the initial and the final flow parameters, in terms of whether shock of a certain type is possible or not. For a given initial and the final set of flow parameters, it is shown that there are in general multiple shock locations. In a third paper (Chakrabarti and Abramowicz, in preparation) we add viscous dissipation in the flow outside shocks.

We use Newtonian hydrodynamics, in particular, we assume the Newtonian model for the central black hole given in terms of the Paczyński and Wiita (1980) potential,

$$\Psi = -\frac{GM}{(r - r_G)} \tag{1}$$

Here, M is the mass of the central object and $r_G = 2GM/c^2$ is its gravitational radius. We assume a polytropic equation of state for the accreted matter, $P = K\rho^{1+1/n}$, where, P and ρ are the isotropic pressure and the matter density respectively, n is the polytropic index (assumed in this paper to be constant throughout the flow, although in general it can vary) and K is related to the specific entropy s: $s = const$ implies $K = const$.

We assume that entropy has constant, but in general different values on either side of the shock. This allows K to change only at the shock.

2 Basic Equations for 1.5D Fluid

Our 1.5D model is based on the two differential equations for two unknown functions: dimensionless radial velocity ϑ and dimensionless sound speed a. Both of these functions are in units of the velocity of light. The equations express radial momentum balance and the mass conservation:

$$\frac{\partial \vartheta}{\partial t} = -\frac{\partial}{\partial x}\left[\frac{1}{2}\vartheta^2 + na^2 + \frac{\lambda^2}{2x^2} + g(x)\right] \tag{2}$$

$$\frac{\partial a}{\partial t} = -\frac{1}{qf(x)a^{q-1}}\frac{\partial}{\partial x}\left[x\vartheta a^q f(x)\right] \tag{3}$$

Here x is the dimensionless radial coordinate in units of r_G, t is dimensionless time in units of (r_G/c), λ is dimensionless angular momentum in units of $(r_G c)$, and q equals $2n+1$ or $2n$ depending on whether the vertical equilibrium is assumed or not. Eqns. (2) and (3) are valid not only for the adiabatic black hole accretion, but for *any* 1.5D or 1D flow in which $g(x)$ is the potential for the radial force (or the rate of the radial momentum deposition) and $f(x)$ is connected with the vertical thickness of the flow $h(x)$:

$$h = \frac{a^{q-2n}f(x)}{x} \tag{4}$$

Two different cases should be discussed separately:

(1) *The shape of the flow is not fixed and vertical equilibrium is assumed*: In this case $q = 2n+1$ and the functions $f(x)$ and $g(x)$ are not independent, but connected by (4) and the vertical equilibrium condition

$$0 = \frac{h^2}{x}\frac{dg}{dx} - na^2 \tag{5}$$

Interdependency of $f(x)$ and $g(x)$ can be seen from,

$$f^2(x) = nx^3(dg/dx)^{-1} \quad \text{and} \quad g(x) = \int \frac{nx^3}{f^2(x)}dx. \tag{6}$$

In particular, with the gravitational potential of the black hole given by eqn. (1) the functions $g(x)$ and $f(x)$ are explicitly given by:

$$g(x) = -\frac{1}{2}(x-1)^{-1}, \tag{7}$$

$$f(x) = x^{3/2}(x-1). \tag{8}$$

When the motion along the vertical direction is small but non-zero, the left-hand side of eqn. (5) becomes $\vartheta((\partial h/\partial x)(\partial h/\partial t)$.

(2) *The shape of the flow is fixed and the vertical equlibrium is not assumed*: In this case $q = 2n$ and the functions $g(x)$ and $f(x)$ are independent, and therefore the flow is strictly speaking only *1D* correct. For example, $g(x)$ given by (7) and $f(x) = x^2$ corresponds to the conical black hole accretion considered by Abramowicz amd Zurek (1981) and Fukue (1987) while $g(x)$ =const corresponds to the flow through a pipe with the dimensionless cross section equal to $f(x)$.

In the stationary case one can trivially integrate the basic equations to get

$$\mathcal{E} = \frac{\vartheta^2}{2} + na^2 + \frac{\lambda^2}{2x^2} + g(x) \tag{9}$$

$$\dot{\mathcal{M}} = x\vartheta a^{2n}h. \tag{10}$$

Here $\mathcal{E}$ is just the total energy and $\dot{\mathcal{M}}$ is connected with the accretion rate.

$$\dot{\mathcal{M}} = \text{const}K^n\dot{M}. \tag{11}$$

The value of the constant depends upon the physical situation given by the choice of the functions $g(x)$ and $f(x)$ and on the dimensional parameters describing the problem. In the case of the black hole accretion

$$\dot{\mathcal{M}} = \frac{(n+1)^n}{16\pi\sqrt{2\pi}}\left(\frac{n+\frac{1}{2}}{n^2}\right)^n \frac{\Gamma(n+\frac{3}{2})}{\Gamma(n+1)}\frac{K^n\dot{M}}{G^2c^{2n-3}M^2}. \tag{12}$$

Here Γ is the Euler gamma function. This can be re-written in terms of the ratio β of the gas pressure to total pressure,

$$\dot{\mathcal{M}} = 4.97 \times 10^{-21} \left(\frac{\dot{M}}{\dot{M}_E}\right) \left(\frac{M_\odot}{M}\right) \frac{(1-\beta)}{\beta^4}. \quad (13)$$

Here $n = 3$ and chemical composition of pure hydrogen was assumed. In the rest of the paper we use $\dot{\mathcal{M}}$ instead of the baryon accretion rate $\dot{M}$. One should remember that $\dot{M}$ is a globally conserved quantity, but $\dot{\mathcal{M}}$ can change through a shock. If no shocks are present $\dot{\mathcal{M}}$ is also a globally conserved quantity for adiabatic flows.

In the case of a shock-free flow, eqns. (2) and (3) provide two conditions for two unknown functions $\vartheta = \vartheta(x; \lambda, \dot{\mathcal{M}}, \mathcal{E})$, and $a = a(x; \lambda, \dot{\mathcal{M}}, \mathcal{E})$ and when λ, $\dot{\mathcal{M}}$, $\mathcal{E}$ are given, these can be solved. However, not all of the solutions are physically acceptable, but only those which pass through a critical point $x = x_c$. The condition for a solution to pass through a critical point can be found in the following (standard) way: Differentiating (9) and (10) one obtains, after eliminating da/dx

$$\frac{d\vartheta}{dx}\left(\vartheta - \frac{2na^2}{q\vartheta}\right) = \frac{2na^2}{q}\frac{d\ln f}{dx} - \frac{dG}{dx} \quad (14)$$

where, $G(x) = g(x) + \lambda^2/2x^2$ is the combined potential. Let us define the critical point $(x = x_c)$ as the place, where

$$\vartheta^2(x_c) = \frac{2n}{q}a^2(x_c) \quad (15)$$

The eqns. (2), and (3) which describe the time dependent behavior of the flow when linearized to obtain the characteristic velocities of small acoustic perturbations, it is found that the two acoustic modes propagate with velocities $a\sqrt{2n/q} \pm \vartheta$. Therefore, the velocity of sound is $a\sqrt{2n/q}$, and from (5) it follows that at the critical point the velocity of the flow equals that of sound. Because very far from the black hole the velocity of the flow is subsonic and at the surface of black hole it is supersonic, equation (15) must be fulfilled for some x. From (14) it then follows that

$$\vartheta^2(x_c) = \left[\frac{dG}{dx}\left(\frac{d\ln f}{dx}\right)^{-1}\right]_{x=x_c} \quad (16)$$

Note, that equation (16), which determines the magnitude of the velocity at the critical point does not depend on the polytropic index n. It depends only on the effective force dG/dx in the direction of motion and on the geometrical term $d\ln f/dx$ which determines the divergence of the fluid flow lines. At a critical point these two terms must have the same sign - this can be called the *generalized de Laval condition* . Special cases of this condition have been derived by various authors: for example, Abramowicz and Zurek (1981) and Lu (1985) for rotating conical accretion flows, Chakrabarti (1986) for rotating general relativistic winds.

The condition for the location of the sonic point (15) and the de Laval condition (16) give two extra restrictions and introduce only one new parameter x_c. Thus, they reduce by one the number of degrees of freedom in the three dimensional parameter space: λ, $\dot{\mathcal{M}}$, $\mathcal{E}$ are not independent, but they must obey a condition

$$F(\lambda, \mathcal{E}, \dot{\mathcal{M}}) = 0. \quad (17)$$

The expression for F can always be found once $f(x)$ and $g(x)$ are provided.

Our basic non-stationary equations (2) and (3) contain no dissipative terms and therefore can be consistent only with the shocks which conserve energy ("Rankin-Hugoniot" shocks). However, the shocks in thin, otherwise dissipation free flows may radiate away energy through their upper and lower surfaces simply because of the presence of the relatively strong heat generation rate. If the length scale in which such radiations occur is small compared to the other length scales (such as the diffusion and cooling) of the flow, one can include such radiative effects by suitable choices of the shock conditions. This we do in the next section.

3 The Shock Conditions

At the shock, the flow velocity must jump from supersonic to subsonic. For black hole accretion this is possible only if the flow passes through a critical point on each side of the shock. A shock is characterized by four *a priori* unknown quantities: possible jumps in the two independent velocities ϑ, a, in the polytropic constant K and in the shock location.

$$\Delta a = a_+(x_s) - a_-(x_s) \tag{18}$$

$$\Delta \vartheta = \vartheta_+(x_s) - \vartheta_-(x_s) \tag{19}$$

$$\Delta K = K_+ - K_- \tag{20}$$

$$x = x_s \tag{21}$$

Here subscripts $-$ and $+$ denote the quantities before and after the shock. Independently of the nature of a shock, the conservation of the fluxes of mass and momentum,

$$\dot{M}_+ = \dot{M}_- \tag{22}$$

$$P_+ + \vartheta_+^2 \rho_+ = P_- + \vartheta_-^2 \rho_- \tag{23}$$

provide two constraints on these four quantities. Since we are dealing with only inviscid flows and the axially symmetric shocks, $\lambda_+ = \lambda_-$ is always fulfilled and gives no constraints. The pre-shock quantities are determined by the outside boundary conditions in the case of accretion flows or by the inner boundary conditions in the case of winds. The after-shock quantities, which are given by $(\lambda_+, \dot{M}_+, \mathcal{E}_+)$, must obey the regularity condition (17) at the critical point after the shock. This provides the third condition for the unknown shock properties. The last, fourth, condition models the nature of the dissipative processes at the shock. We would like to stress that the shocks considered here have upper and lower "surfaces" located at $z = \pm h(x_s)$. Radiation emitted through these surfaces carries away some energy and entropy from the flow. Therefore, these

shocks differ qualitatively from the "Rankin-Hugoniot" shocks discussed in the standard text books (e.g., Landau and Lifshitz, 1959) in the way the fourth condition, connected with dissipation, are formulated. We propose to consider three distinct possibilities for the fourth condition corresponding to three extreme physical situations: Rankin-Hugoniot shocks ($\mathcal{E}_+ = \mathcal{E}_-$), isentropic compression waves ($K_+ = K_-$), and isothermal shocks ($a_+ = a_-$). These three types of shock are schematically presented in Figure 1. In the following we discuss briefly the nature of these shocks. Paper II provides the complete discussion of them.

In Rankin-Hugoniot shocks no energy is radiated away through the surface of the flow at the shock location, i.e., the radiative cooling mechanism is extremely inefficient. Because the post-shock temperature is higher, the sound speed and therefore the thickness of the disk are greater than their pre-shock values. For this type of shock $\mathcal{E}_+ = \mathcal{E}_-$, but $T_+ > T_-$, and $s_+ > s_-$. In the context of black-hole accretion shocks of this type have been studied by Hawley (1986), and Fukue (1987) and others.

In isentropic compression waves the entropy of the flow does not change in the flow but some energy is lost at the 'shock'. The amount of entropy generated at the shock front is comparable to the entropy radiated away. This type corresponds to the exactly opposite of the Rankin-Hugoniot case and is therefore important to study. For this type of shock $s_+ = s_-$ but $\mathcal{E}_+ < \mathcal{E}_-$, and $T_+ > T_-$.

In isothermal shocks radiative cooling is very efficient. Some energy and entropy are lost from the surface of the flow at the shock location to keep the post-shock temperature equal to its pre-shock value. (If the shock triggers some exoergic reaction then both the energy and the entropy may be *generated* instead.) This implies that the sound speed and the thickness of the flow remain unchanged through the shock. For this type of shock $T_+ = T_-$, but $\mathcal{E}_+ < \mathcal{E}_-$, and $s_+ < s_-$. or $\mathcal{E}_+ > \mathcal{E}_-$, and $s_+ > s_-$.

We shall see later that *any* dissipation processes at the shock can be described as a combination of just *two* (not three) of the possibilities mentioned above in the sense that the fourth shock condition can be formally written as:

$$A(\mathcal{E}_+ - \mathcal{E}_-) - B(\dot{\mathcal{M}}_+ - \dot{\mathcal{M}}_-) = 0. \tag{24}$$

This can be considered the most general shock condition. For a given set of the initial parameters choosing the ratio A/B from $-\infty$ to $+\infty$ one recovers all the possible shock solutions.

4 Black Hole Accretion and Winds in 1.5D model

4.1 Shock Free Solutions

We now specialize to the case of a rotating geometrically thin disc with non-dissipative accretion or winds and with hydrostatic equilibrium in the transverse direction. We also confine our attention to the case where the polytropic index n is equal to 3. In this case, as already mentioned, the functions $g(x)$ and $f(x)$ are given by,

$$g(x) = -\frac{1}{2(x-1)}, \tag{25}$$

and

$$f(x) = x^{\frac{3}{2}}(x-1). \tag{26}$$

With these functions, the critical point conditions become (with $n = 3$),

$$a_c{}^2 = \frac{7}{6}\vartheta_c{}^2, \tag{27}$$

and

$$\vartheta_c{}^2 = \frac{2(x_c-1)}{x_c^2}\frac{(\lambda^2{}_K(x_c) - \lambda^2)}{(5x_c-3)}. \tag{28}$$

Since $\vartheta_c{}^2$ is always greater than zero, the angular momentum at the critical point must be *less* than the Keplerian value. The energy of the flow $\mathcal{E}_c$ with angular momentum λ and passing through a critical point at x_c is given by,

$$\mathcal{E}_c = \frac{\lambda^2}{2x_c^2}\left[1 - \frac{16(x_c-1)}{5x_c-3}\right] + \frac{4x_c}{(x_c-1)(5x_c-3)} - \frac{1}{2(x_c-1)}, \tag{29}$$

or, inversely,

$$\lambda^2 = \left[\mathcal{E}_c - \frac{3}{2}\frac{(x_c+1)}{(x_c+1)(5x_c-3)}\right]\frac{2x_c^2(5x_c-3)}{(13-11x_c)}. \tag{30}$$

Fig. 2a shows the variation of λ^2 with x_c for a range of flow energy $\mathcal{E}_c$. Notice that for $0 \leq \mathcal{E}_c \leq \mathcal{E}_*(= 0.01718)$ there are three critical points, as was also shown by Abramowicz and Zurek (1981) for conical flows. For $\mathcal{E} > \mathcal{E}_*$ the flow has only the innermost critical point. The outermost and innermost critical points are 'X' types and the middle one is 'O' type. Two 'X' type critical points can, in principle, allow two local stationary transonic solutions; however, only one of them can join the black hole horizon to the large distance (Lu and Abramowicz, 1988; Anderson, 1988). Also shown are the curves for the Keplerian angular momentum distribution λ_K, for the flow with marginally stable energy $\mathcal{E}_{ms} = -1/16$ (this touches the Keplerian curve at $x_c = x_{ms} = 3.0$,) and the locus of the extrema of the curves. A similar diagram is drawn for various accretion rates $\dot{\mathcal{M}}$ in Fig. 2b. In this case one also has a critical accretion rate $\dot{\mathcal{M}}_*$ above which flow passes through only the innermost critical point. The lower limit of the accretion rate in a transonic flow is, of course, 0 which corresponds to $\lambda = \lambda_K$.

4.2 Solutions Including Shocks

A shock connects flows with two sets of parameters $(\lambda, \dot{\mathcal{M}}, \mathcal{E})$ for each of which the flow must be transonic. The nature of this connection in different types of shocks mentioned in the previous section can be understood from Fig. 3. Here we draw $\dot{\mathcal{M}}$ *vs.* $\mathcal{E}$ curve for a given angular momentum ($\lambda = 1.7$ for illustration purposes) and schematically show the nature of the various shock transitions. The branches AMB, BC and CMD correspond to the loci of the innermost 'X' type critical points, the middle 'O' type critical points, and the outermost 'X' type critical points respectively.

In the case of the Rankin-Hugoniot shocks, the shock transitions are horizontal. In accretion, the flow with lower entropy (belonging to the branch MD) passes through the outer critical point and the post shock flow with higher entropy (belonging to the branch MB) passes through the inner critical point. In winds, the flow with lower entropy (belonging to the branch MA) passes through the inner critical point and the post shock flow with higher entropy (belonging to the branch MC) passes through the outer critical point. In Fig. 3, a_1a_2 and w_1w_2 are representatives of such shock transitions in accretion and winds respectively. The difference of $\dot{M}$ between points such as a_1 and a_2 (or, between w_1 and w_2) directly determines the entropy change in accretion (or winds).

In the case of isentropic shocks the transitions are vertical. In accretion, the flow with higher energy (belonging to the branch MD) passes through the outer critical point and the post shock flow with lower energy (belonging to the branch MB) passes through the inner critical point. In winds, the flow with higher energy (belonging to the branch MA) passes through the inner critical point and the post shock flow with lower energy (belonging to the branch MC) passes through the outer critical point. In Fig. 3, a_3a_4 and w_3w_4 are representatives of such shocks in accretion and winds respectively. The difference of $\mathcal{E}$ between points such as a_3 and a_4 (or, between w_3 and w_4) directly determines the energy jump in accretion (or winds).

It is obvious that combining the vertical and the horizontal transitions described above one can produce any possible transition. Thus, the shock condition (24) is the most general one. However, we discuss the isothermal shocks separately below since

their physical meaning is clear.

In the case of isothermal shocks the shock transitions are oblique. In accretion, the flow with higher energy and entropy (belonging to the branch MC) passes through the outer critical point and the post shock flow with lower energy and entropy (belonging to the branch MB) passes through the inner critical point. In winds, the flow with higher energy and entropy (belonging to the branch MA) passes through the outer critical point and the post shock flow with lower energy and entropy (belonging to the branch MD) passes through the inner critical point. In Fig. 3, a_5a_6 and w_5w_6 are representatives of such shocks in accretion and winds respectively. The difference of $(\mathcal{E}, \dot{M})$ between points such as a_5 and a_6 (or, between w_5 and w_6) directly determines the energy and entropy jump in accretion (or winds).

Figs. 4a-c describe *schematically* the nature of pre-shock and post-shock flows which may participate in shocks. The Mach number of the flow is plotted against the logarithmic radial distance. Types of flows depicted in Figs. 4a-b may participate in all three shocks but the type described in Fig. 4c can participate only in isothermal shocks. For obvious reasons we call them xα, αx and $\alpha\alpha$ type diagrams respectively. For Rankin-Hugoniot shocks the curves are contours of constant accretion rate and for isentropic compression waves or isothermal shocks the curves are of constant energy. In all the cases the symbols I and O indicate flow passing through the inner and the outer critical points respectively, and the jump from s_1 to s_2 (shown by dark circles) represents a typical shock transition. In isothermal shocks both the energy and the accretion rate change, and therefore a shock transition can be possible by combining two α type flows (Fig. 4c). Although the shock transitions determine the post-shock parameters uniquely, it is not essential that the shock location is determined uniquely. This was discussed by several authors (e.g., Habbal and Tsinganos 1983, Fukue 1987, Paper II). Note that in the case of a flow in which the functions $f(x)$ and $g(x)$ are assumed to be independent one can produce an arbitrary number of shocks at prescribed locations by an appropriate choice of functions $f(x)$ and $g(x)$.

5 Concluding Remarks

In a fully consistent dissipative and non-stationary hydrodynamical model one should be able to describe the formation of stationary shocks in a unique way, so the resulting standing shock properties and locations depend only upon the boundary conditions. Shocks in our non-dissipative and stationary model are not uniquely determined by the boundary conditions, as they also depend on the arbitrary choice of the coefficients A, B which appear in the shock condition (24). This arbitrariness summarizes our lack of knowledge of dissipative and non-stationary processes. The most natural way to reduce this arbitrariness would be to study the stability properties of our model and to add a small dissipation outside shocks: (a) The addition of small dissipation may produce entropy differentially at each shock location. The application of the Prigogine principle of least entropy production may then help to lift the 'degeneracy' of the shock locations. (b) It is possible that some shocks are inherently unstable. We have found that for shock free solutions, two stable acoustic modes exist which propagate upstream and downstream. For the solutions with shocks three modes are present which may render some shocks unstable. Brief results on the local stability analysis are presented in Paper II. Detailed properties will be discussed elsewhere.

The study of non-stationary flow is important for yet another reason. We have demonstated that any flow, which starts far away from the hole with a subsonic accretion velocity can be stationary only if its initial energy, angular momentum and the accretion rate are connected by an exact regularity condition (17). However, in a typical astrophysical situation these three quantities are *independently* fixed. In the case of a

galactic black hole in a binary system they are fixed by the binary parameters and the evolutionary status of the normal star, while in the case of a black hole in an active galactic nucleus by the properties of the host galaxy. This means that the stationary solutions describing black hole accretion of rotating matter (at least when dissipation is small) are astrophysically rare. Typical black hole accretion must be non-stationary: Abramowicz and Zurek (1981), Abramowicz, Livio, and Lu (1986), suggested that a bistable oscillation between 'high' and 'low' states should be expected. In the numerical models of Hawley (1986) no bistable oscillation was present possibly because the flow at the outer boundary was supersonic and only post-shock flow passed through a critical point. It is still unclear if flows with proper boundary conditions do show bistability. This issue is under investigation by Trussoni, Chakrabarti and Abramowicz (in preparation).

In this paper we have described all the stationary solutions corresponding to rotating, axially symmetric, polytropic, dissipation free black hole accretion and winds. We have pointed out the possibility of the most general type of axially symmetric, standing shocks and briefly discussed three generic types of shocks (Rankin-Hugoniot, isoentropic and isothermal) which correspond to three extreme cases of dissipation at the shock. Detail description of the properties of the shocks in terms of the flow parameters are discussed in Paper II.

Acknowledgments

The authors would like to thank Professor Abdus Salam, the International Atomic Energy Agency and UNESCO for hospitality at the International Centre for Theoretical Physics, Trieste.

REFERENCES

Abramowicz, M.A., Livio, M., and Lu, J.F., 1986, in *Proc. of the Fourth Marcel Grossman Meeting on General Relativity*, R. Ruffini, (Ed.), Elsevier Science Publishers, B.V.

Abramowicz, M.A. and Zurek, W. H. 1981, *Ap. J.*, **246**, 314.

Anderson, M., 1988, *M. N. R. A. S.*, (submitted).

Chakrabarti, S.K., 1986, *Ap. J.*, **303**, 582.

Chakrabarti, S.K., 1988, *Ap. J.*, (submitted, Paper II).

Chang, K.M., and Ostriker, J.P., 1985, *Ap. J.* **288**, 428.

Ferrari, A., Trussoni, E., Rosnar, R., and Tsinganos, K., 1985, *Ap. J.*, **294**, 397.

Fukue, J. 1987, *Publ. Astron. Soc. Japan*, **39**, 309.

Habbal, S. R. and Tsinganos, K. 1983, *J. Geophys. Res.*, **88**, 1965.

Hawley, J. W 1986, *Numerical Astrophysics*, J. Centerella (Ed.), Cambridge Univ. Press., UK.

Hawley, J.W., Smarr, L. and Wilson, J. 1984, *Ap. J.*,**277**, 296.

Kaisig, M., 1988, *Astron. Astr.*, (submitted).

Landau, L.D., and Lifshitz, F.D. 1959, *Fluid Mechanics*, Pargamon press, (New York).

Lu, J.F. 1985,*Astron. Ap.*, **148**, 176.

Lu, J.F. and Abramowicz, M.A., 1988, *Acta Astrophys. Sinica* **8**, 1.

Paczyński, B. and Wiita, P.J. 1980, *Astr. Ap.*, **88**, 23.

Sawada, K., Matsuda, T., and Hachisu, I. 1986, *M. N. R. A. S.* , **219**, 75.

Spruit, H.C. 1987, *Astron. Ap.*, **184**, 173.

FIGURE CAPTIONS

Fig . 1: Three types of standing shocks: a) Rankin-Hugoniot shock, where the effective cooling processes are so inefficient that no energy is lost from the surface, b) compression waves where entropy generated at the shock is comparable to the amount radiated away. c) isothermal shocks where the cooling processes are so efficient that the post-shock internal energy (and thickness) remains same as the pre-shock values. In this case both the energy and the entropy must be radiated away (or generated) in order to keep the flow isothermal. The shocks are indicated by heavy vertical black lines.

Fig. 2ab: Variation of λ^2 with the location of the critical points for (a) a set of energies, and (b) a set of accretion rates. The energies for which the plots drawn were, from top to bottom: $-1/16$ (dotted), $\mathcal{E}_K$ (dot-dashed), -0.0065, 0.0, 0.0065, 0.013, $\mathcal{E}_* = 0.01718$ (dashed), and 0.025. The large dotted curve passes through the extrema of all of the curves. The accretion rates for which the plots drawn were, from top to bottom: 0.0 (dot-dashed), 0.5, 1.0, 1.5, 2.0, $\dot{M}_* = 2.73$ (dashed), and 3.5. ($\dot{M}$ is written in units of 10^{-5}.) For energies higher than $\mathcal{E}_*$ or accretion rates higher than $\dot{M}_*$ there is only one critical point in the flow.

Fig. 3: Variation of energy of the transonic flow with the accretion rate for a given angular momentum. The branches AMB, BC and CMD are the loci of the outer 'X' type critical points, middle 'O' type critical points and the inner 'X' type critical points respectively. Typical shock transitions connecting pairs of parameters are also shown. a) a_1a_2 and w_1w_2 represent Rankin-Hugoniot shocks in accretion and winds, b) a_3a_4 and w_3w_4 represent isentropic compression waves in accretion and winds. c) a_5a_6 and w_5w_6 represent isothermal shocks in accretion and winds.

Fig. 4(a-c): Variation of the Mach number of the transonic flow is *schematically* shown against the radial distance from the hole. I and O indicate the pre-shock and the post-shock flows, a jump from s_1 to s_2 represents a typical shock transition. A pair of curves drawn in 4ab ($x\alpha$ and αx types respectively) may participate in all three kinds of shocks, but curves drawn in 4c ($\alpha\alpha$) participate only in isothermal shocks.

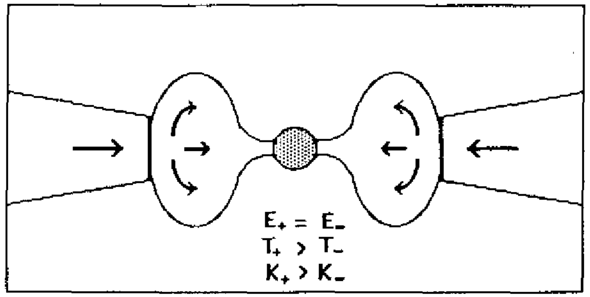

(a)

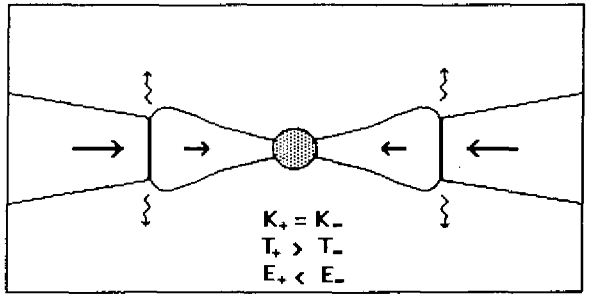

(b)

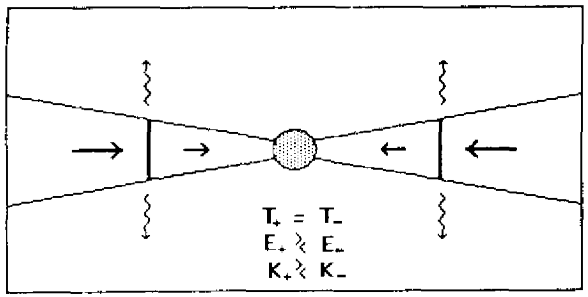

(c)

Fig. 1

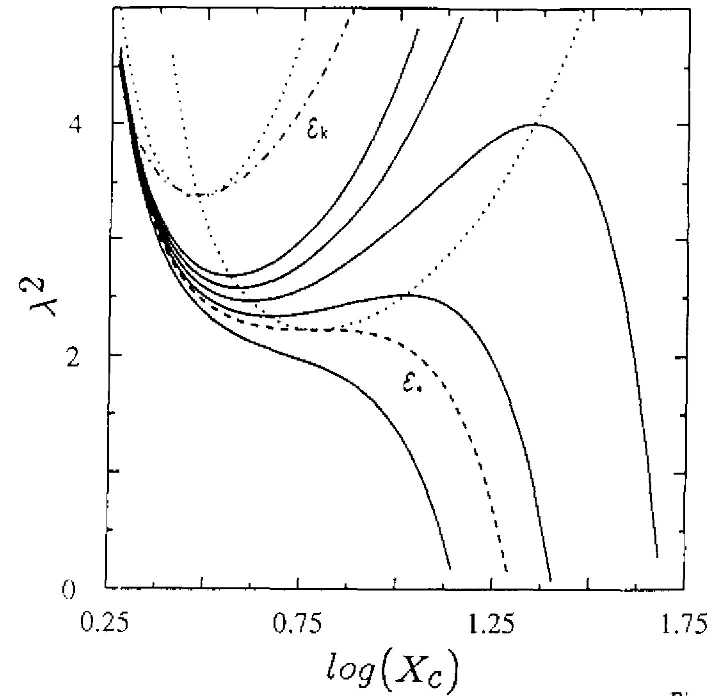

Fig. 2a

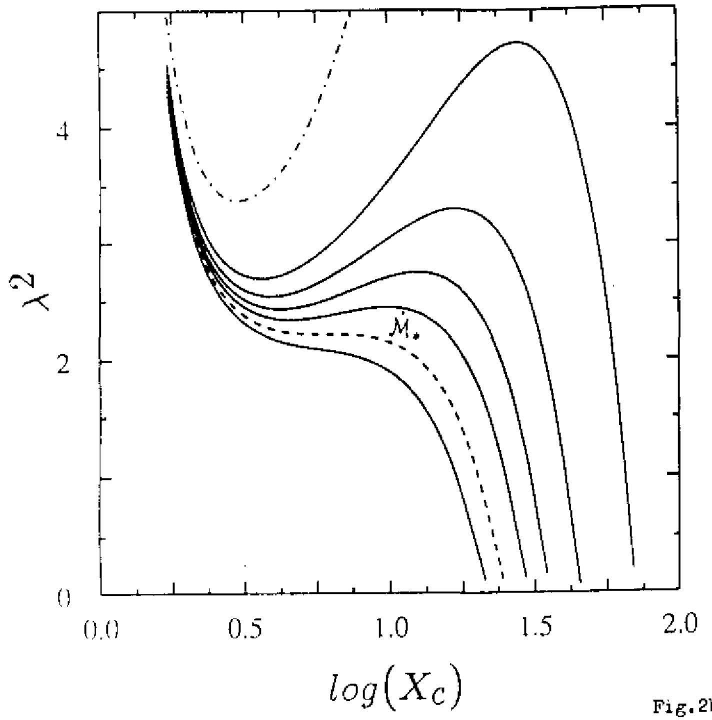

4
2
0
0.0
0.5
1.0
1.5
2.0
λ^2
$\dot{M}_*$
$log(X_c)$

Fig.2b

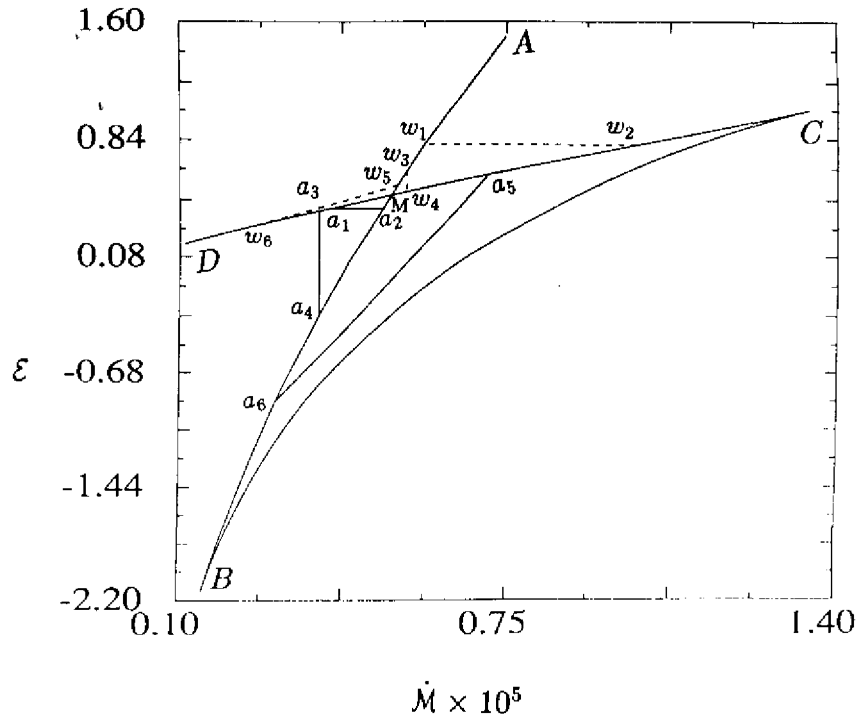

1.60
0.84
0.08
-0.68
-1.44
-2.20
0.10
0.75
1.40
A
B
C
D
M
w_1
w_2
w_3
w_4
w_5
w_6
a_1
a_2
a_3
a_4
a_5
a_6
$\mathcal{E}$
$\dot{M} \times 10^5$

Fig. 3

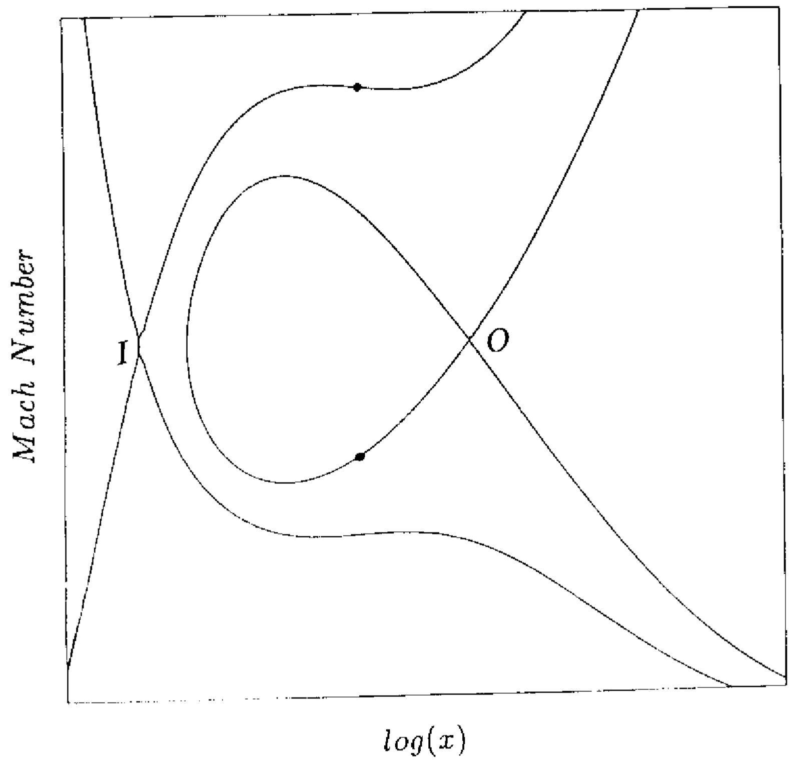

Fig. 4a

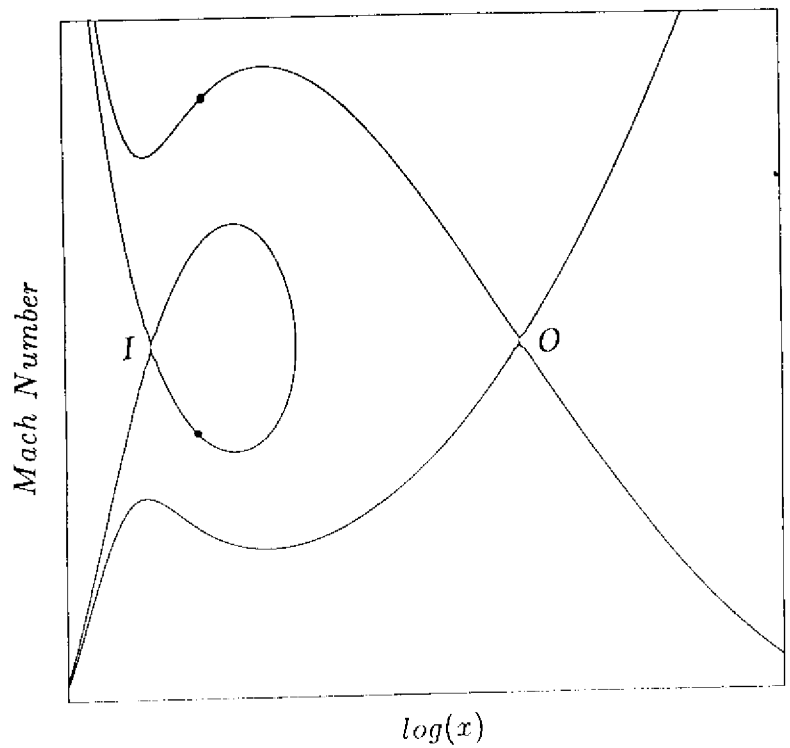

Fig.4b

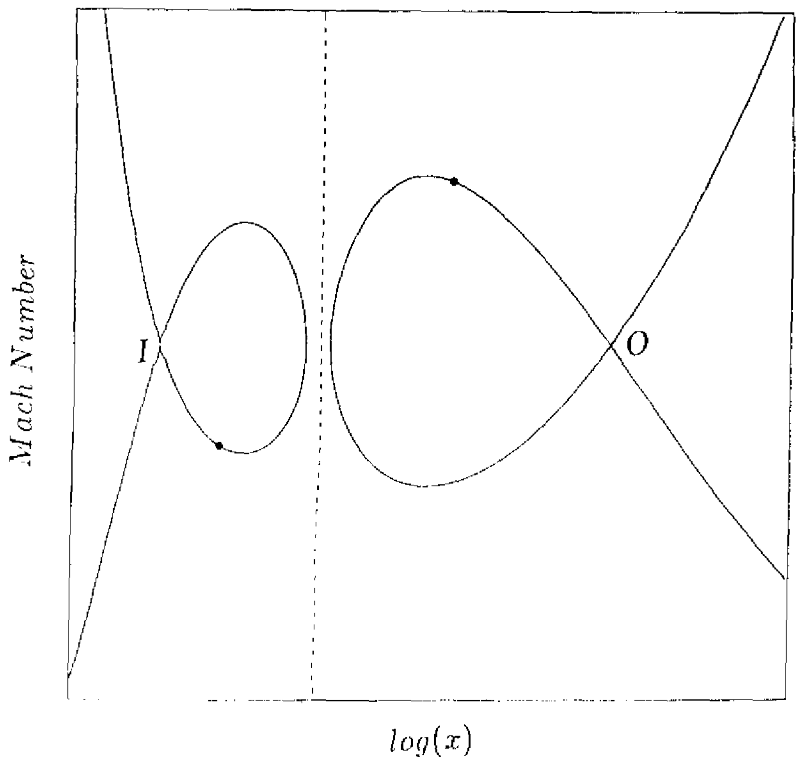

Fig.4c

Stampato in proprio nella tipografia
del Centro Internazionale di Fisica Teorica